Genetic and dietary regulation of lipid droplet expansion in *Caenorhabditis elegans*

Shaobing O. Zhang[a], Andrew C. Box[a], Ningyi Xu[a], Johan Le Men[a], Jingyi Yu[a], Fengli Guo[a], Rhonda Trimble[a], and Ho Yi Mak[a,b,1]

[a]Stowers Institute for Medical Research, Kansas City, MO 64110; and [b]Department of Molecular and Integrative Physiology, University of Kansas Medical Center, Kansas City, KS 66160

Edited by Cynthia Kenyon, University of California, San Francisco, CA, and approved January 25, 2010 (received for review October 26, 2009)

Dietary fat accumulates in lipid droplets or endolysosomal compartments that undergo selective expansion under normal or pathophysiological conditions. We find that genetic defects in a peroxisomal β-oxidation pathway cause size expansion in lipid droplets that are distinct from the lysosome-related organelles in *Caenorhabditis elegans*. Expansion of lipid droplets is accompanied by an increase in triglycerides (TAG) that are resistant to fasting- or TAG lipase-triggered lipolysis. Nevertheless, in mutant animals, a diet poor in vaccenic acid reduced the TAG level and lipid droplet size. Our results implicate peroxisomal dysfunction in pathologic lipid droplet expansion in animals and illustrate how dietary factors modulate the phenotype of such genetic defects.

peroxisome | β-oxidation | *daf-22* | *dhs-28* | *maoc-1*

Lipid droplets are the primary site of storage for neutral lipids such as triglycerides (TAG) and cholesterol esters (1–3). In metazoans, the number and size of lipid droplets vary in different tissues, and lipid droplets undergo dynamic changes that reflect the metabolic status and dietary intake of the organism. Proliferation of white adipocytes and excessive TAG storage in enlarged lipid droplets during adipocyte differentiation correlate with obesity in mammals (4–6). In neutral lipid-storage diseases, where the gene encoding the adipose triglycerides lipase is mutated, large intracellular lipid droplets accumulate in non-adipose tissues (7). These observations suggest tissue- and nutrient-specific regulation of lipid droplets. Lipid accumulation also can occur in endolysosomal compartments in pathophysiological conditions, such as in foam cells in atherosclerotic plaques (8). However, the mechanisms that govern the subcellular distribution and mobilization of lipids are not well understood.

Fasting induces mobilization of fatty acids from lipid-storage compartments. To release the energy stored in the form of fatty acids, the fatty acids are broken down sequentially through β-oxidation to yield acetyl-CoA that then can be fed into the Krebs cycle (Fig. 1) (9). In metazoans, β-oxidation occurs in mitochondria and peroxisomes where multiple parallel pathways with overlapping substrate specificities are used (9). We and others have identified enzymes encoded by the *C. elegans* genome that may act in mitochondrial or peroxisomal β-oxidation (10, 11).

In *C. elegans*, the intestine and hypodermis serve as sites of fat storage that are regulated by nutrient availability through conserved insulin, TGF-β, serotonin, and mammalian target of rapamycin (mTOR) signaling pathways (12–16). The intestinal cells are endowed with multiple vesicular compartments (17–19) in which different classes of lipids may be stored in distinct sites. Lipophilic dye staining using Nile Red previously suggested a role for lysosome-related organelles (LROs), also known as "gut granules," in fat storage (20). However, a recent report suggested that most neutral lipids also could be stored in Nile Red staining-negative vesicular structures (21). Accordingly, genetic mutants that fail to form LROs have normal TAG level (20). These observations prompted our hypothesis that an alternative fat-storage compartment for neutral lipids exists in *C. elegans*. Here, we report the identification in *C. elegans* of intracellular lipid droplets that expand in mutants that accumulate high levels of TAG because of peroxisomal dysfunction. In addition, we provide evidence on how dietary factors may modulate directly the lipid droplet size in *C. elegans*.

Results

Peroxisomal Dysfunction Causes Lipid Droplet Expansion. Using a fluorescently labeled fatty acid C1-BODIPY-C12 to visualize lipid-storage compartments, we conducted a forward genetic screen for mutants with enlarged lipid droplets. We recovered in total 11 alleles that fell into four complementation groups. Molecular cloning revealed four genes annotated to regulate peroxisomal function or peroxisomal matrix protein import, namely *maoc-1*, *dhs-28*, *daf-22*, and *prx-10.* The *dhs-28* and *daf-22* genes encode enzymes responsible for the last two steps of peroxisomal β-oxidation, whose human orthologues control the catabolism of straight-chain and branched-chain fatty acids (BFCA) and the processing of bile acids. DHS-28/dehydrogenase and DAF-22/thiolase also have a role in processing the fatty acid moiety of the *C. elegans* dauer pheromone (22). The *maoc-1* gene encodes a hydratase that acts upstream of DHS-28 (Fig. 1 and Fig. S1). The *maoc-1*, *dhs-28*, and *daf-22* mutant animals show intense staining of C1-BODIPY-C12 that accumulates in enlarged spherical intracellular structures (Fig. 2 *A–D*). Oil-Red-O staining confirmed that the enlarged spherical intracellular structures in the mutant intestine are indeed sites of fat storage (Fig. 2 *E* and *F*). Ultrastructural studies revealed that these spherical compartments resemble lipid droplets found in other organisms (23), which are bound by a phospholipid monolayer (Fig. 2*G* and Fig. S2). We conclude that a block in peroxisomal β-oxidation causes selective expansion of lipid droplets in *C. elegans*.

A rescuing transgene of *maoc-1* driven by its endogenous promoter indicates that, like *dhs-28* and *daf-22*, *maoc-1* is strongly expressed in the intestine (Fig. 2 *H* and *I*). Next, we addressed whether the expanded lipid droplets in *maoc-1(lf)* animals could be dissipated upon reexpression of the MAOC-1 enzyme. Indeed, transient expression of the wild-type but not a mutant form of MAOC-1 in the late-larval L4 and young-adult stages reduced the size of lipid droplets (Fig. 2 *J–M*). Our results suggest that lipid droplet size in *C. elegans* is dynamic and is linked intimately to storage, mobilization, and peroxisomal catabolism of fat.

A loss-of-function allele of *prx-10* defined the fourth complementation group in our screen for lipid droplet expansion mutants (Fig. 2 *N* and *O* and Fig. S1). The *C. elegans* PRX-10 protein is the orthologue of human PEX10, a highly conserved

Author contributions: S.O.Z. and H.Y.M. designed research; S.O.Z., A.C.B., N.X., J.L.M., J.Y., F.G., R.T., and H.Y.M. performed research; S.O.Z. and H.Y.M. analyzed data; and S.O.Z. and H.Y.M. wrote the paper.

The authors declare no conflict of interest.

This article is a PNAS Direct Submission.

Freely available online through the PNAS open access option.

[1]To whom correspondence should be addressed. E-mail: hym@stowers.org.

This article contains supporting information online at www.pnas.org/cgi/content/full/0912308107/DCSupplemental.

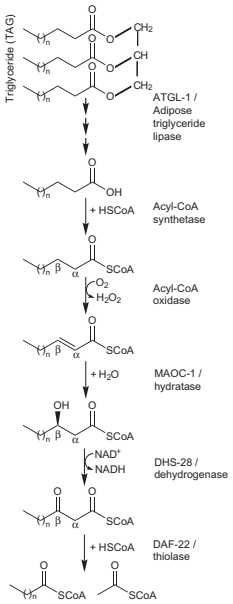

Fig. 1. Fatty acid catabolism by the MAOC-1/DHS-28/DAF-22 peroxisomal β-oxidation pathway in *C. elegans*.

RING finger protein required for the import of peroxisomal matrix proteins (24–26). In *prx-10(hj21)* mutant animals, a monomeric red fluorescent protein (mRFP) bearing the canonical type-1 peroxisomal targeting signal (PTS1), or a GFP-tagged DAF-22/thiolase fusion protein were retained in the cytoplasm (Fig. 2 *P–S*). These results indicate that proper targeting of the peroxisomal β-oxidation enzymes is necessary for their function. Furthermore, mutations that compromise peroxisome biogenesis or function cause lipid droplet expansion in *C. elegans*, similar to that observed in neutral lipid-storage diseases in humans.

Lipid Droplet Expansion Is Modulated by Diet. We found that the lipid droplet expansion phenotype in *C. elegans* peroxisomal β-oxidation mutants can be modulated by different *E. coli* diets. When *dhs-28(lf)* animals were grown on HB101 instead of OP50 *E. coli* lawns, the abundance of enlarged lipid droplets was reduced (Fig. 3 *A* and *B*). We measured the diameter and extrapolated the volume of all BODIPY-labeled intracellular structures in the second intestinal segment by confocal microscopy and 3D reconstruction. The BODIPY-labeled structures <3 μm in diameter were likely to be primarily LROs, which remained constant when *dhs-28(lf)* animals were fed either diet (Fig. S3). However, we observed a significant decrease in the number and proportion of BODIPY-positive structures that were >3 μm in diameter when *dhs-28(lf)* animals were fed HB101 instead of OP50 (Fig. S3). As a result, the total volume of BODIPY-positive structures was reduced by 43% (Fig. 3*C*), largely because of the decreased number of lipid droplets that were >4 μm in diameter (Fig. 3*D*).

We next asked if the suppression of lipid droplet expansion in *dhs-28(lf)* animals fed the HB101 diet was associated with a change in particular lipid species. Total lipids were extracted from wild-type and mutant animals and separated by thin-layer chromatography (TLC). A strong correlation was observed between TAG level and the abundance and size of lipid droplets: *dhs-28* and *maoc-1* mutants had higher levels of TAG than wild-type animals; mutant or wild-type animals had lower TAG levels when fed HB101 than when fed OP50 (Fig. 3*E*). We examined fatty acid compositions (Fig. 4) and quantified TAG levels by gas chromatography-mass spectrometry (GC-MS). On the OP50 diet, *dhs-28* mutants accumulated 61% more TAG than wild-type animals (Fig. 5*A*). A 4.6-fold decrease in TAG level was observed when *dhs-28(lf)* animals were fed HB101 (*dhs-28*/HB101) rather than OP50 (*dhs-28*/OP50) (Fig. 5*A*). Such decrease is not caused by a change in the feeding rates of these animals (Fig. S4). Our results indicate that the accumulation of excess TAG and expansion of lipid droplets are regulated by both genetic and dietary factors.

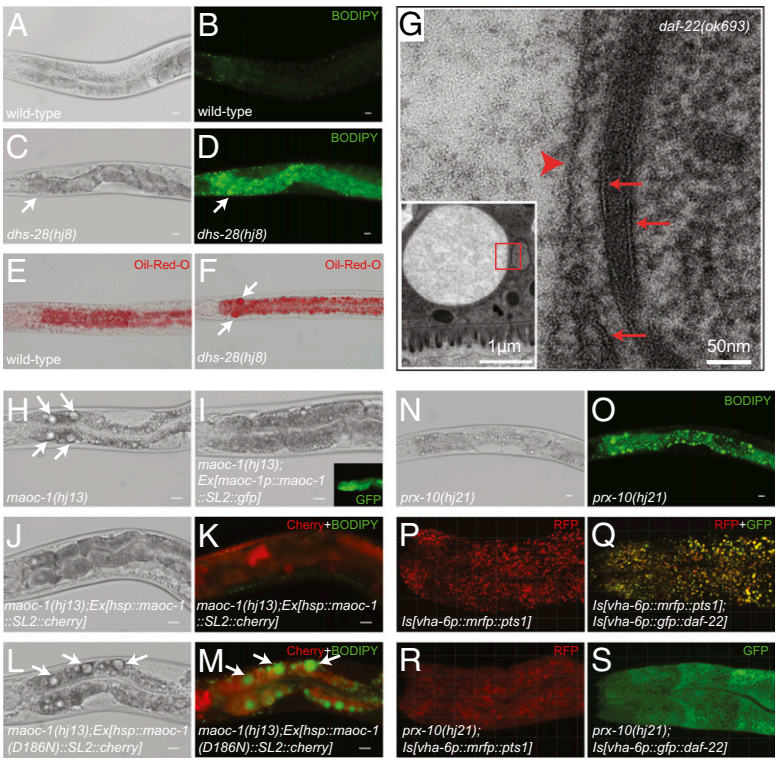

Fig. 2. Enlarged lipid droplets caused by defective peroxisomal β-oxidation or peroxisomal matrix protein import. Bright-field images and BODIPY images of 1-day-old adult wild-type (*A* and *B*) and *dhs-28(hj8)* animals (*C* and *D*) are shown. (*E* and *F*) Oil-Red-O staining of L4 wild-type and *dhs-28(hj8)* animals. Enlarged spherical structures are indicated by arrows. (*G*) Electron micrograph showed that an expanded lipid droplet (boxed area in *Inset*) had phospholipid monolayer (arrowhead) as opposed to phospholipid bilayer (arrows) of nearby organelles. The intestinal lumen is at the bottom of the inset. (*H*) In a 1-day-old adult *maoc-1* worm, lipid droplets were >10 μm in diameter (arrows). (*I*) A *maoc-1(hj13);Ex[maoc-1p::maoc-1::SL2::gfp]* worm had no expanded droplet visible at the same age. *maoc-1* was expressed in the intestine based on GFP expression (*Inset*). (*J* and *K*) A 2-day-old adult *maoc-1;Ex[hsp::maoc-1::SL2::cherry]* worm that was heat shocked at L4 and 1-day-old adult stages showed no large droplet in bright-field (*J*) or BODIPY (*K*) images. In *K*, transgenic coexpression marker Cherry is in red. (L and *M*) Control 2-day-old adult *maoc-1;Ex[hsp::maoc-1(D186N)::SL2::cherry]* worm retained large lipid droplets (arrows). (*N* and *O*) Lipid droplet expansion in a 1-day-old adult *prx-10(hj21)* animal. **(*P*)** Three-dimensional projection of confocal stacks showed the punctate signal of mRFP::PTS1, which colocalized with GFP::DAF-22 (*Q*). (*R*) Cytoplasmic retention of mRFP::PTS1 and GFP::DAF-22 (*S*) in *prx-10* mutant background. (Scale bars in *A–D* and *H–O*, 20 μm. Grid lines in *P–S*, 10 μm.)

GENETICS

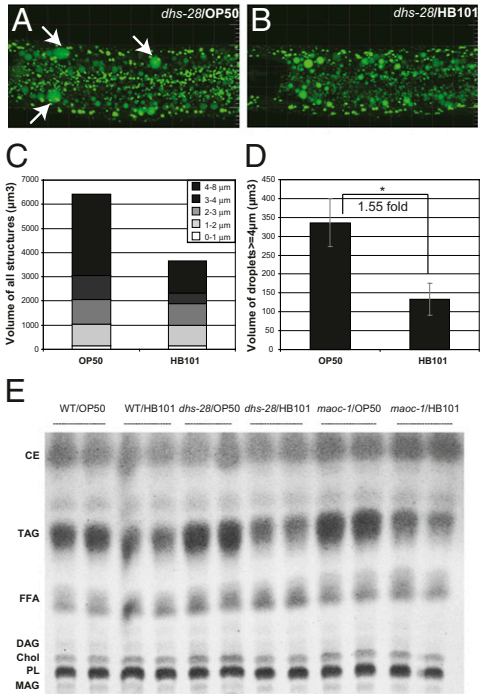

Fig. 3. Dietary regulation of lipid droplet expansion. (*A* and *B*) Late-stage L4 *dhs-28* mutants on the OP50 diet accumulated more expanded lipid droplets (arrows) than *dhs-28* mutants on the HB101 diet. Images are from 3D projections of BODIPY fluorescence confocal Z-stacks. (Grid lines, 10 µm.) All BODIPY-positive structures in the second gut segment of 10 worms on each diet were counted and measured for diameters. (*C*) Volumes of BODIPY-stained structures were calculated for each diameter sector (n = 10 for each diet). (*D*) Volume of BODIPY-stained structures with diameters >4 µm (mean ± SEM; *, $P < 0.05$). (*E*) TLC analysis of total lipids extracted from wild-type (WT), *dhs-28(hj8)*, and *maoc-1(hj13)* animals equivalent to 100 µg total soluble protein. Results of two of six replicates of each genotype/diet experiment are presented. CE, cholesterol ester; Chol, cholesterol; DAG, diacylglycerol; FFA, free fatty acids; MAG, monoacylglycerol; PL, phospholipids; TAG, triacylglycerol.

Dietary Vaccenic Acid Modulates Lipid Droplet Expansion. *C. elegans* obtains fatty acids from *E. coli* (27) or by de novo synthesis, elongation, and desaturation (28, 29). We wondered if particular fatty acid species in the *E. coli* diet contribute to lipid droplet expansion in *C. elegans* peroxisomal mutants. Using GC-MS, we compared the fatty acid composition of HB101 and OP50 and the total fatty acid and TAG fatty acid compositions of *dhs-28* mutants grown on the two diets. The relative abundance of C16:0 and C18:2n6 was significantly lower and of C18:0 and C18:1n7 was significantly higher in OP50 than in HB101 (Fig. 4*A*). We found that the high relative abundance of vaccenic acid (C18:1n7) in OP50 was specifically mirrored in both total fatty acid composition and TAG fatty acid composition in *dhs-28(lf)* (Fig. 4 *B* and *C* and Fig. S5) and wild-type animals (Fig. S6). The relatively low abundance of vaccenic acid in HB101 could be one factor contributing to lower TAG levels and fewer enlarged lipid droplets in *dhs-28*/HB101 animals. To test this hypothesis, *dhs-28* mutants were cultivated on HB101 plates supplemented or not supplemented with vaccenic acid. Compared with *dhs-28*/HB101 animals, the animals cultivated on plates supplemented with vaccenic acid (*dhs-28*/HB101/V) had a 43% increase in total volume of BODIPY-labeled structures (Fig. 4 *D–G*); this increase could be attributed solely to a significant increase in the number of lipid droplets >4 µm in diameter and a corresponding 1.35-fold increase in lipid droplet volume. Furthermore, *dhs-28*/HB101/V animals had an elevated representation of vaccenic acid in TAG, similar to that of *dhs-28*/OP50 animals (Fig. 4*C*), and, importantly, a 29% increase in total TAG level (Fig. 5*A*). Thus, vaccenic acid supplementation partially restored the TAG level, and more specifically the abundance of lipid droplets >4 µm in diameter, in HB101-fed *dhs-28(lf)* animals. We conclude that a diet poor in vaccenic acid may reduce the severity of phenotype in peroxisome-defective animals that are genetically predisposed to store excessive TAG in large lipid droplets.

Enlarged Lipid Droplets in Peroxisomal Mutants Are Resistant to Lipolysis. Fasting induces TAG hydrolysis. However, this process is severely impaired when peroxisomal β-oxidation is defective in *C. elegans*. Fasting reduced the TAG level by 5.9-fold in wild-type animals (Fig. 5*A*). In contrast, a 1.6-fold reduction was observed in fasted *dhs-28* mutants, which retained large lipid droplets in intestinal cells (Fig. 5 *A* and *B*). Adipose triglyceride lipase-1 (ATGL-1) is a major lipase for fat mobilization from lipid droplets in mammals and *Drosophila* (30, 31) and from fat-storage compartments in *C. elegans* dauers (32). Overexpression of an ATGL-1::GFP fusion protein under the control of *atgl-1* promoter reduced the TAG level in wild-type and *dhs-28(lf)* animals, albeit to a lesser extent in the latter (Fig. 5*A*). However, a substantial amount of TAG remained in *dhs-28(lf)* animals, correlating with the retention of large lipid droplets despite correct targeting of ATGL-1::GFP to their surface (Fig. 5 *C* and *D*). The inability of ATGL-1::GFP to mobilize TAG from large droplets was not caused by different protein levels of ATGL-1::GFP in mutant versus wild-type animals (Fig. S7). Analysis of remnant TAG from *dhs-28(lf)* animals that underwent fasting-induced or ATGL-1–mediated lipolysis revealed overrepresentation of vaccenic acid, C18:2n6, and C19:Δ fatty acids when compared with wild-type animals (Fig. 5*E*). Preferential retention of these long-chain fatty acids in TAG suggests that they may be the primary substrates of the MAOC-1/DHS-28/DAF-22 β-oxidation pathway in *C. elegans*.

In *dhs-28* mutants, the lipolysis-resistant compartment includes the enlarged lipid droplets that have a distinct origin from the Nile Red-positive LROs. The number of Nile Red-positive LROs is severely reduced in *glo* mutants (19). However, large lipid droplets remained in *daf-22;glo-4* double mutants (Fig. 5*F*). In addition, a GLO-1::GFP fusion protein, which localized to LROs (20), was not found on the surface of expanded lipid droplets (Fig. 5 *G* and *H*). These results suggest that in both wild-type and *dhs-28(lf)* animals fat is stored in both ATGL-1–sensitive and ATGL-1–resistant compartment(s). Furthermore, lipid droplets and LROs are distinct fat-storage compartments in *C. elegans*.

We initially explored whether ATGL-1 overexpression could stimulate TAG hydrolysis and reduce lipid droplet size in *dhs-28* mutants. Surprisingly, concurrent blocking of peroxisomal β-oxidation and overexpression of ATGL-1 caused developmental arrest as early as the first larval stage (Fig. 5 *I* and *J*). The incidence of such synthetic larval arrest correlated with the severity of the lipid droplet expansion phenotype, because an HB101 diet partially suppressed larval arrest (Fig. 5*I*). Reduction of transgenic expression of the ATGL-1::GFP fusion protein by RNAi suppressed synthetic larval arrest, confirming the specificity of the phenotype (Fig. 5*I*). Our results suggest that in peroxisome-defective mutants, sequestration of TAG in enlarged lipid droplets limits the pool of ATGL-1 hydrolysable fat that ultimately slows larval development. When ATGL-1 is overexpressed, premature depletion of fat then causes synthetic larval arrest. Alternatively, peroxisomal mutant animals might be more susceptible to lipotoxicity, triggered by the release of free fatty acid from TAG by ATGL-1 overexpression.

Discussion

In this paper, we report the identification of intracellular lipid droplets in *C. elegans* and their selective expansion in peroxisome-

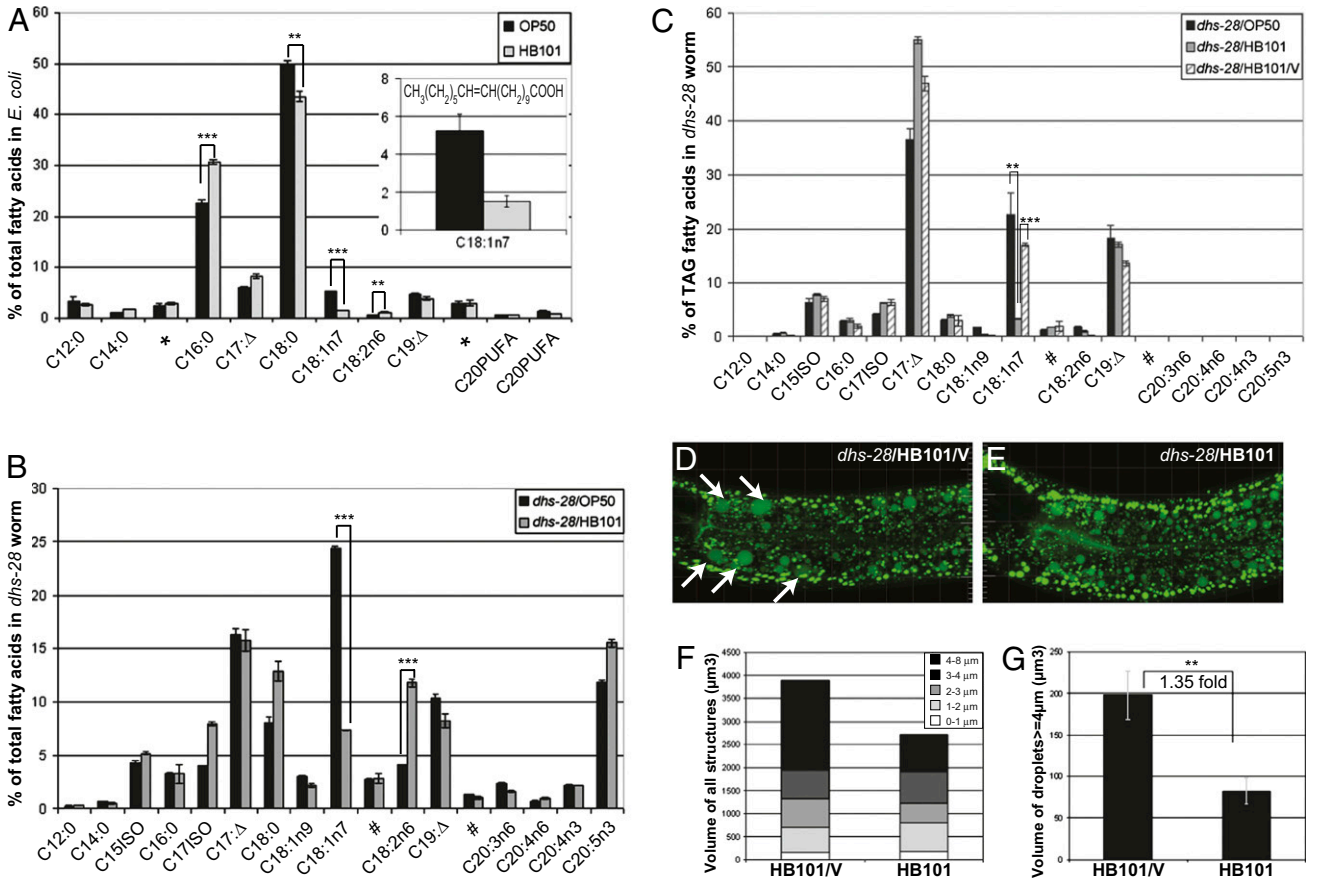

Fig. 4. Regulation of lipid droplet expansion by dietary vaccenic acid. (*A*) Total fatty acid compositions of OP50 and HB101 *E. coli*. OP50 and HB101 differed significantly in the levels of saturated C16:0, C18:0, monounsaturated C18:1n7, and di-unsaturated C18:2n6 fatty acids. *Inset* shows a magnified view of C18:1n7 (vaccenic acid) data. *, unidentified fatty acid species. (*B*) Total fatty acid composition of *dhs-28(lf)* animals on the OP50 or HB101 diet. *dhs-28*/OP50 and *dhs-28*/HB101 differed significantly in the levels of C18:1n7 and C18:2n6. **#**, unidentified fatty acid species. (*C*) TAG fatty acid composition of *dhs-28(lf)* animals on OP50, HB101, or vaccenic acid-supplemented HB101 diets. *dhs-28*/OP50 and *dhs-28*/HB101 differed significantly in the level of C18:1n7 in TAG. Supplementation of vaccenic acid increased its percentage in TAG. Data in *A–C* are mean ± SD of three independent samples. (*D* and *E*) Vaccenic acid supplementation of HB101 diet increased the abundance of expanded lipid droplets (arrows) in late-stage L4 *dhs-28(lf)* animals. V, vaccenic acid supplementation. Images are from 3D projection of BODIPY fluorescence Z-stacks. (Grid lines, 10 μm.) (*F*) Vaccenic acid supplementation increased the total volume of BODIPY-labeled structures ($n = 10$ animals), especially those with diameters >4 μm (mean ± SEM, $n = 20$ animals) (*G*). For all statistical analyses: **, $P < 0.01$; ***, $P < 0.001$.

defective mutants. Our results suggest an evolutionarily conserved role of the MAOC-1/DHS-28/DAF-22 peroxisomal β-oxidation pathway in unmethylated long-chain fatty acid catabolism that modulates lipid droplet size. Mutations in the human orthologues of these genes cause severe peroxisomal disorders, i.e., D-bifunctional protein (DBP) deficiency(OMIM 261515) and autosomal adrenoleukodystrophy (ALD) (OMIM 202370), that result in neurodegeneration and neonatal death, as in other peroxisome biogenesis disorders (33, 34). However, we did not observe overt neurological defects in the *C. elegans* mutants, perhaps because *C. elegans* neurons are not myelinated. Instead, these mutants share a common phenotype of intracellular lipid droplet expansion caused by excessive accumulation of TAG. The enlarged lipid droplets persisted in fasted animals or when ATGL-1 triglyceride lipase was overexpressed. This persistence suggests an intriguing cross-talk between peroxisomes and the lipid droplets: Defective peroxisomal β-oxidation inhibits TAG hydrolysis in lipid droplets. Such cross-talk may protect against lipotoxicity when free fatty acid released from lipid droplets cannot be catabolized by defective peroxisomes. The mechanism of peroxisome–lipid droplet cross-talk is not known, but we noted clusters of peroxisomes adjacent to the surface of enlarged lipid droplets in *daf-22* mutant animals, suggesting that a physical interaction between these organelles may be necessary. A similar model of physical and functional coupling of peroxisomes with lipid droplets has been proposed in budding yeast (35).

In our genetic screen, we used C1-BODIPY-C12 as a probe to identify mutant animals that showed intense BODIPY fluorescence from grossly enlarged intracellular structures. These structures were not marked by the LRO marker GLO-1::GFP (Fig. 5*H*) or endosomal markers GFP::RAB-5 and GFP::RAB-7 (Fig. S8). Instead, they were bona fide lipid droplets that were surrounded by a phospholipid monolayer (Fig. 2*G*). Furthermore, the overexpressed TAG lipase ATGL-1::GFP was targeted to the lipid droplet surface in *dhs-28(lf)* animals (Fig. 5*D*). Taken together, our results suggest that in wild-type animals, vesicular structures marked by ATGL-1::GFP might be lipid droplets that are largely distinct from Nile Red-positive LROs (Fig. 5*C* and Fig. S7).

We note that the properties of C1-BODIPY-C12 are not identical to those of Nile Red. For example, C1-BODIPY-C12 appears to mark both LROs and lipid droplets, at least in the peroxisomal mutants. Unlike Nile Red, C1-BODIPY-C12 clearly stains the hypodermis and early embryos in utero. The staining of early embryos in utero suggests that ingested C1-BODIPY-C12 is incorporated into endogenous fat, which is exported from the intestine to the oocytes (36). Nevertheless, we agree with a

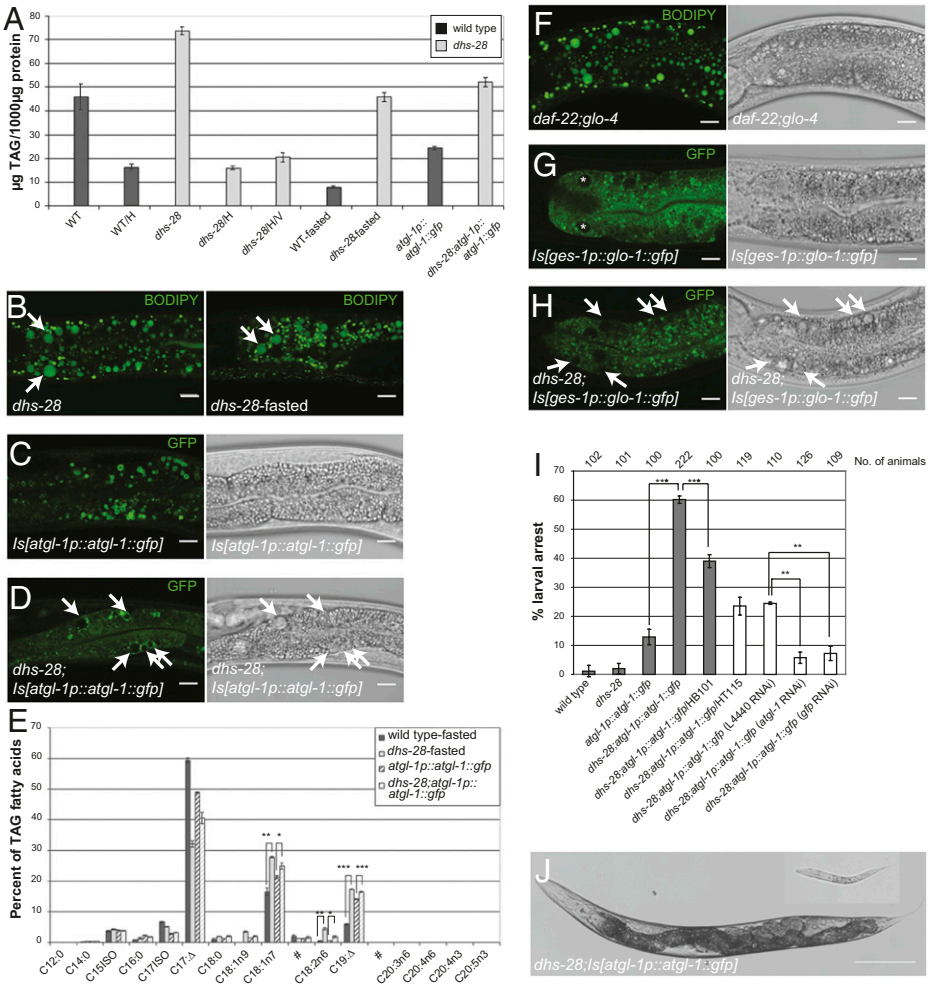

Fig. 5. Enlarged lipid droplets are resistant to fasting- and ATGL-1–induced lipolysis. (*A*) Quantification of TAG from late-stage L4 animals (equivalent to1,000 µg protein) under various conditions. Default diet was OP50 unless indicated otherwise. Fasted, animals had been fasted in M9 buffer with constant agitation for 24 h since late L4 stage; H, HB101 diet; H/V, HB101 diet with vaccenic acid supplementation; WT, wild type. Data are mean ± SEM of three independent samples. (*B*) In fasted *dhs-28(lf)* animals, expanded lipid droplets remained (arrows). (*C*) Expression of *atgl-1::gfp* driven by *atgl-1* promoter (*hjIs67*). In a wild-type L4 animal, ATGL-1::GFP protein localized to spherical structures. (*D*) ATGL-1::GFP protein localized to the surface of large lipid droplets in *dhs-28(lf)* animals (arrows). (*E*) Fatty acid compositions of remnant TAG resulting from fasting- or ATGL-1–induced lipolysis were different in wild-type and *dhs-28(lf)* animals. Data are mean ± SD of three independent samples. (*F*) Enlarged lipid droplets remained in L4 *daf-22 (ok693);glo-4(ok623)* mutants. (*G*) Localization of GLO-1::GFP to LROs in wild-type animals. Nuclei of intestinal cells are marked by asterisks. (*H*) GLO-1::GFP did not localize to the surface of expanded lipid droplets (arrows) in *dhs-28(lf)* animals. (*I*) Larval arrest under different conditions. Data are mean ± SD of three independent plates, and the total number of animals scored for each strain is indicated. HT115, HT115 *E. coli*; V, vaccenic acid. (*J*) Examples of a nonarrested and an arrested (*Inset*) *dhs-28;atgl-1p::atgl-1::gfp* animal. (Scale bars, 10 µm in *B–D* and *F–H*; 200 µm in *J*.) For all statistical analyses: *, $P < 0.05$, **, $P < 0.01$; ***, $P < 0.001$.

recent report that observations based on dye-staining methods in live or fixed animals should be verified by biochemical measurement of lipids (21).

In mammals, the peroxisomal β-oxidation pathways catabolize dietary very-long-chain fatty acids [VLCFA, carbon (C) >20] and branched-chain fatty acids (BCFA) (34). A block in peroxisomal β-oxidation in *C. elegans* may cause elevated levels of VLCFA, which can be stored as TAG in lipid droplets. However, BCFA and VLCFA are absent in the *E. coli* diet of *C. elegans*. We did not detect fatty acid with chain length longer than C19 in the TAG of *dhs-28* (Fig. 4*C* and Fig. S5) or wild-type animals (Fig. S6). Furthermore, in contrast to another report (37), the total fatty acid composition and TAG fatty acid composition of *dhs-28(lf)* and wild-type animals were similar when fed an OP50 or HB101 diet (compare Fig. 4 *B* and *C* and Fig. S6). Thus, excess VLCFAs are unlikely to cause TAG accumulation and lipid droplet expansion in *C. elegans* peroxisomal β-oxidation mutants.

Abnormal lipid droplets are observed in hepatocytes and neurons in human patients with DBP deficiency, and it has been suggested that male sterility in a knock-out mouse model correlated with the appearance of large lipid droplets in the testes (38–40). We propose that common factors in mammalian and *C. elegans* diets contribute to lipid droplet expansion in mutants with peroxisomal defects. Such factors are unlikely to be BCFA or VLCFA, because they are absent in the *E. coli* diet of *C. elegans*. Our results suggest an ancient role of the peroxisomal MAOC-1/DHS-28/DAF-22 pathway in the catabolism of long-chain fatty acids, such as vaccenic acid, which is present in all diets. Absorption and subsequent blocking of vaccenic acid catabolism contributes to lipid droplet expansion in *dhs-28(lf)* animals, whereas feeding on HB101 *E. coli* poor in vaccenic acid reduces lipid droplet size in these animals. Because vaccenic acid supplementation of HB101 did not fully recapitulate the effect of OP50 diet on lipid droplet expansion and TAG level, additional metabolites in OP50 also may modulate fat storage and compartmentalization in mutant animals.

Treatment for peroxisome biogenesis disorders in humans usually is aimed at decreasing the level of VLCFA; this level is regulated by peroxisomal β-oxidation. Thus far, limited success in dietary intervention has been reported, in part because of a lack of suitable metazoan models for systematic analysis of dietary factors that can modulate the phenotypes caused by peroxisomal defects. It is unclear how lipid droplet expansion in nonadipose tissues may contribute to the pathology of DBP deficiency or ALD. Nevertheless, reduction of dietary long-chain fatty acid may be considered as an additional strategy for treating patients with peroxisomal disorders. We also propose that *C. elegans* peroxisome-defective mutants may serve as models for high-throughput identification of additional dietary factors and small molecules that are therapeutic for peroxisomal disorders.

Methods

Strains and Transgenes. The wild-type strain was Bristol N2. All animals were raised at 20 °C. The following alleles and transgenes were used:

LGII: *maoc-1(hj13), maoc-1(hj14), daf-22(ok693)*

LGIII: *prx-10(hj21)*
LGV: *glo-4(ok623)*
LGX: *dhs-28(hj8)*
hjIs9[ges-1p::glo-1::gfp], hjIs37[vha-6p::mrfp::pts1], hjIs67[atgl-1p::atgl-1::gfp], hjIs73[vha-6p::gfp::daf-22], pwIs72[vha-6p::gfp::rab-5], pwIs170[vha-6p::gfp::rab-7]

hjIs9, *hjIs37*, and *hjIs73* were generated by microparticle bombardment. *hjIs67* was generated by integration of an extrachromosomal array using UV irradiation. All strains were outcrossed with N2 at least twice.

Genetic Screening and Mapping. Genetic screening for mutants with enlarged lipid droplets was described previously (22). Genetic mapping was performed based on an SNP-based mapping strategy by crossing the mutants with the Hawaiian *C. elegans* isolate CB4856 (41, 42). We mapped *hj13* to LGII between snp_K05F1[1] and snp_T05A6[1]. We chose *maoc-1* as a candidate gene for sequencing, and we identified missense mutations for both *hj13* and *hj14* (Fig. S1). The lipid droplet phenotype of *hj13* was rescued by a *maoc-1p::maoc-1::SL2::gfp* transgene. We mapped *hj21* to LGIII between snp_haw43040 and snp_haw43202. Transformation with groups and individual cosmids indicated that the cosmid C34E10 contained the gene mutated in *hj21* (five of eight lines). We sequenced the gene C34E10.4 and identified a G-to-A mutation that destroyed the splice donor site of intron 3. We named the gene *prx-10* based on its homology to human PEX10 (Fig. S1).

Additional experimental procedures can be found in *SI Methods*.

ACKNOWLEDGMENTS. We thank Hao Zhu for advice in lipid analysis; Eyleen O'Rourke, Alex Soukas, and Gary Ruvkun for comments and for communicating unpublished results; Andy Fire (Stanford University School of Medicine, Stanford, CA) and Mario de Bono (Medical Research Council, Laboratory of Molecular Biology, Cambridge, UK) for vectors; Malcolm Parker, Robb Krumlauf, Ron Yu, and Matt Gibson for comments; Joe Mercado for providing a transgenic strain; and the Stowers Institute Microscopy Center for assistance. Some nematode strains used in this work were provided by the Caenorhabditis Genetics Center, which is funded by the National Institutes of Health National Center for Research Resources. This work was supported by the Stowers Institute for Medical Research and in part by Research Grant 5-FY07-662 from the March of Dimes Foundation.

1. Martin S, Parton RG (2006) Lipid droplets: A unified view of a dynamic organelle. *Nat Rev Mol Cell Biol* 7:373–378.
2. Ducharme NA, Bickel PE (2008) Lipid droplets in lipogenesis and lipolysis. *Endocrinology* 149:942–949.
3. Goodman JM (2008) The gregarious lipid droplet. *J Biol Chem* 283:28005–28009.
4. Faust IM, Johnson PR, Stern JS, Hirsch J (1978) Diet-induced adipocyte number increase in adult rats: A new model of obesity. *Am J Physiol* 235:E279–E286.
5. Rodeheffer MS, Birsoy K, Friedman JM (2008) Identification of white adipocyte progenitor cells in vivo. *Cell* 135:240–249.
6. Slavin BG (1979) Fine structural studies on white adipocyte differentiation. *Anat Rec* 195:63–72.
7. Fischer J, et al. (2007) The gene encoding adipose triglyceride lipase (PNPLA2) is mutated in neutral lipid storage disease with myopathy. *Nat Genet* 39:28–30.
8. Schmitz G, Grandl M (2009) Endolysosomal phospholipidosis and cytosolic lipid droplet storage and release in macrophages. *Biochim Biophys Acta* 1791:524–539.
9. Reddy JK, Hashimoto T (2001) Peroxisomal beta-oxidation and peroxisome proliferator-activated receptor alpha: An adaptive metabolic system. *Annu Rev Nutr* 21:193–230.
10. Mak HY, Nelson LS, Basson M, Johnson CD, Ruvkun G (2006) Polygenic control of *Caenorhabditis elegans* fat storage. *Nat Genet* 38:363–368.
11. Van Gilst MR, Hadjivassiliou H, Jolly A, Yamamoto KR (2005) Nuclear hormone receptor NHR-49 controls fat consumption and fatty acid composition in *C. elegans*. *PLoS Biol* 3:e53.
12. Greer ER, Pérez CL, Van Gilst MR, Lee BH, Ashrafi K (2008) Neural and molecular dissection of a *C. elegans* sensory circuit that regulates fat and feeding. *Cell Metab* 8: 118–131.
13. Kimura KD, Tissenbaum HA, Liu Y, Ruvkun G (1997) daf-2, an insulin receptor-like gene that regulates longevity and diapause in *Caenorhabditis elegans*. *Science Y* 277: 942–946.
14. Sze JY, Victor M, Loer C, Shi Y, Ruvkun G (2000) Food and metabolic signalling defects in a *Caenorhabditis elegans* serotonin-synthesis mutant. *Nature* 403:560–564.
15. Ashrafi K, et al. (2003) Genome-wide RNAi analysis of *Caenorhabditis elegans* fat regulatory genes. *Nature* 421:268–272.
16. Soukas AA, Kane EA, Carr CE, Melo JA, Ruvkun G (2009) Rictor/TORC2 regulates fat metabolism, feeding, growth, and life span in *Caenorhabditis elegans*. *Genes Dev* 23: 496–511.
17. Leung B, Hermann GJ, Priess JR (1999) Organogenesis of the *Caenorhabditis elegans* intestine. *Dev Biol* 216:114–134.
18. Chen CC, et al. (2006) RAB-10 is required for endocytic recycling in the *Caenorhabditis elegans* intestine. *Mol Biol Cell* 17:1286–1297.
19. Hermann GJ, et al. (2005) Genetic analysis of lysosomal trafficking in *Caenorhabditis elegans*. *Mol Biol Cell* 16:3273–3288.
20. Schroeder LK, et al. (2007) Function of the *Caenorhabditis elegans* ABC transporter PGP-2 in the biogenesis of a lysosome-related fat storage organelle. *Mol Biol Cell* 18: 995–1008.
21. O'Rourke EJ, Soukas AA, Carr CE, Ruvkun G (2009) *C. elegans* major fats are stored in vesicles distinct from lysosome-related organelles. *Cell Metab* 10:430–435.
22. Butcher RA, et al. (2009) Biosynthesis of the *Caenorhabditis elegans* dauer pheromone. *Proc Natl Acad Sci USA* 106:1875–1879.
23. Tauchi-Sato K, Ozeki S, Houjou T, Taguchi R, Fujimoto T (2002) The surface of lipid droplets is a phospholipid monolayer with a unique fatty acid composition. *J Biol Chem* 277:44507–44512.
24. Okumoto K, et al. (1998) Mutations in PEX10 is the cause of Zellweger peroxisome deficiency syndrome of complementation group B. *Hum Mol Genet* 7:1399–1405.
25. Warren DS, Morrell JC, Moser HW, Valle D, Gould SJ (1998) Identification of PEX10, the gene defective in complementation group 7 of the peroxisome-biogenesis disorders. *Am J Hum Genet* 63:347–359.
26. Thieringer H, Moellers B, Dodt G, Kunau WH, Driscoll M (2003) Modeling human peroxisome biogenesis disorders in the nematode *Caenorhabditis elegans*. *J Cell Sci* 116:1797–1804.
27. Perez CL, Van Gilst MR (2008) A ^{13}C isotope labeling strategy reveals the influence of insulin signaling on lipogenesis in *C. elegans*. *Cell Metab* 8:266–274.
28. Brock TJ, Browse J, Watts JL (2006) Genetic regulation of unsaturated fatty acid composition in *C. elegans*. *PLoS Genet* 2:e108.
29. Kniazeva M, et al. (2003) Suppression of the ELO-2 FA elongation activity results in alterations of the fatty acid composition and multiple physiological defects, including abnormal ultradian rhythms, in *Caenorhabditis elegans*. *Genetics* 163:159–169.
30. Grönke S, et al. (2005) Brummer lipase is an evolutionary conserved fat storage regulator in *Drosophila*. *Cell Metab* 1:323–330.
31. Zimmermann R, et al. (2004) Fat mobilization in adipose tissue is promoted by adipose triglyceride lipase. *Science* 306:1383–1386.
32. Narbonne P, Roy R (2009) *Caenorhabditis elegans* dauers need LKB1/AMPK to ration lipid reserves and ensure long-term survival. *Nature* 457:210–214.
33. Steinberg SJ, et al. (2006) Peroxisome biogenesis disorders. *Biochim Biophys Acta* 1763:1733–1748.
34. Wanders RJ, et al. (2001) Peroxisomal fatty acid alpha- and beta-oxidation in humans: Enzymology, peroxisomal metabolite transporters and peroxisomal diseases. *Biochem Soc Trans* 29:250–267.
35. Binns D, et al. (2006) An intimate collaboration between peroxisomes and lipid bodies. *J Cell Biol* 173:719–731.
36. Grant B, Hirsh D (1999) Receptor-mediated endocytosis in the *Caenorhabditis elegans* oocyte. *Mol Biol Cell* 10:4311–4326.
37. Joo HJ, et al. (2009) *Caenorhabditis elegans* utilizes dauer pheromone biosynthesis to dispose of toxic peroxisomal fatty acids for cellular homoeostasis. *Biochem J* 422: 61–71.
38. Ferdinandusse S, et al. (2006) Clinical and biochemical spectrum of D-bifunctional protein deficiency. *Ann Neurol* 59:92–104.
39. Huyghe S, Mannaerts GP, Baes M, Van Veldhoven PP (2006) Peroxisomal multifunctional protein-2: The enzyme, the patients and the knockout mouse model. *Biochim Biophys Acta* 1761:973–994.
40. Huyghe S, et al. (2006) Peroxisomal multifunctional protein 2 is essential for lipid homeostasis in Sertoli cells and male fertility in mice. *Endocrinology* 147:2228–2236.
41. Wicks SR, Yeh RT, Gish WR, Waterston RH, Plasterk RH (2001) Rapid gene mapping in *Caenorhabditis elegans* using a high density polymorphism map. *Nat Genet* 28: 160–164.
42. Davis MW, et al. (2005) Rapid single nucleotide polymorphism mapping in *C. elegans*. *BMC Genomics* 6:118.